AD-A133 322 LIMITING ENERGY SPREAD AT HIGH LASER INTENSITIES USING PHASE SPACE DISPLACEMENT(U) KMS FUSION INC ANN ARBOR MI H TAKEDA ET AL. 25 AUG 83 KMSF-U1360 N00014-80-C-0614 1/1

UNCLASSIFIED F/G 20/5 NL

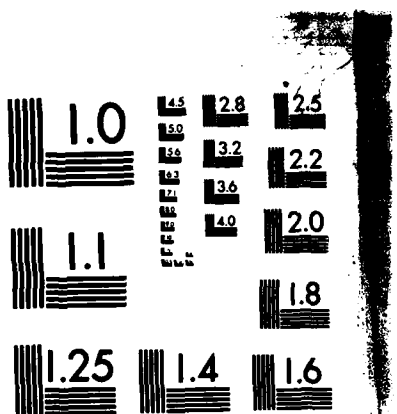

KMSF-U1360

kms fusion inc.

LIMITING ENERGY SPREAD AT HIGH LASER INTENSITIES USING PHASE SPACE DISPLACEMENT

H. Takeda and S. B. Segall

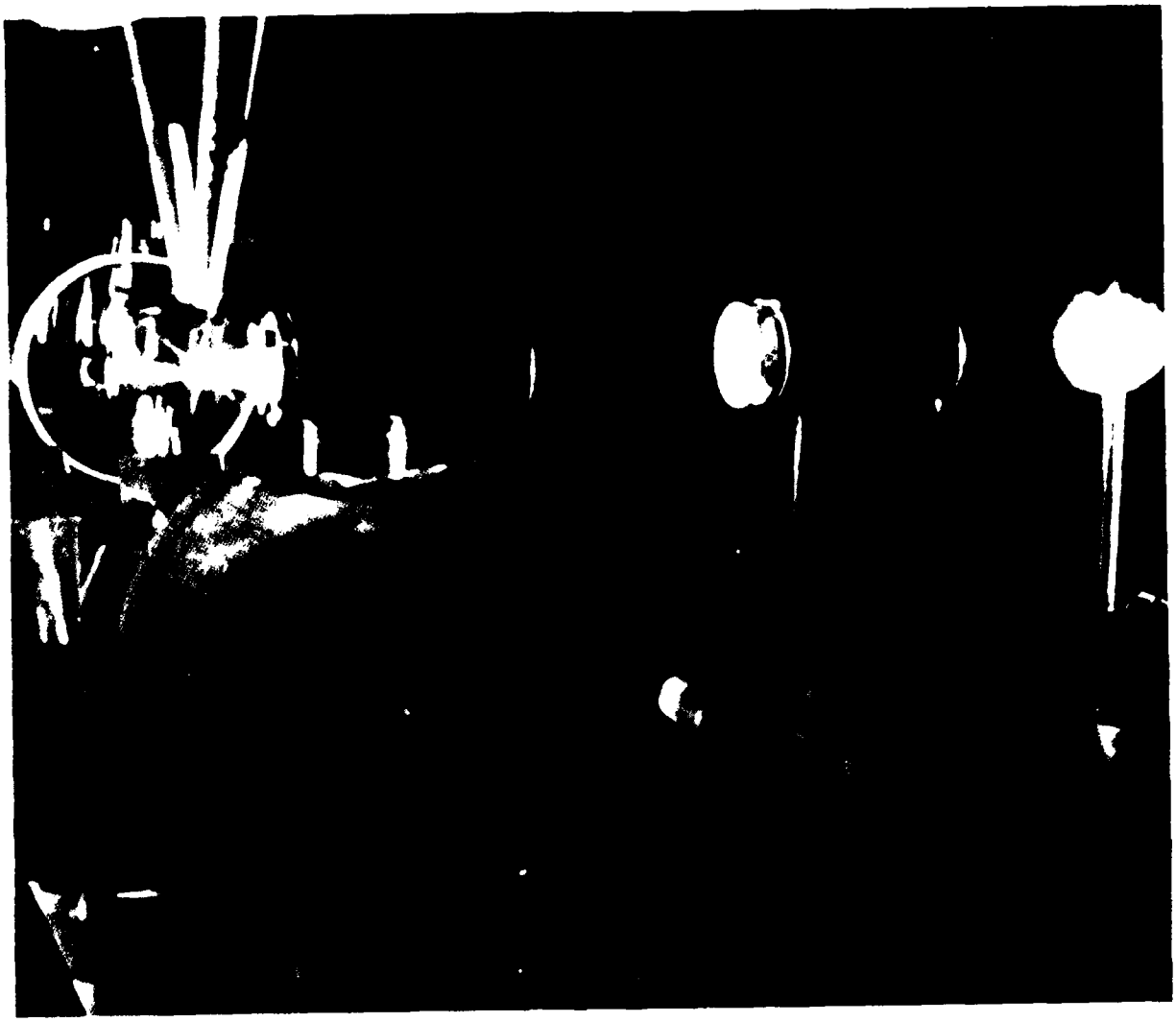

SECURITY CLASSIFICATION OF THIS PAGE (When Data Entered)

REPORT DOCUMENTATION PAGE

READ INSTRUCTIONS BEFORE COMPLETING FORM

1. REPORT NUMBER: KMSF-U1360	2. GOVT ACCESSION NO. AD-A133 322
3. RECIPIENT'S CATALOG NUMBER	
4. TITLE (and Subtitle): Limiting energy spread at high laser intensities using phase space displacement	5. TYPE OF REPORT & PERIOD COVERED: Technical Report
	6. PERFORMING ORG. REPORT NUMBER
7. AUTHOR(s): H. Takeda and S. B. Segall	8. CONTRACT OR GRANT NUMBER(s): N00014-80-C-0614
9. PERFORMING ORGANIZATION NAME AND ADDRESS: KMS Fusion, Inc. 3621 South State Rd., P.O. Box 1567 Ann Arbor, MI 48106	10. PROGRAM ELEMENT, PROJECT, TASK AREA & WORK UNIT NUMBERS
11. CONTROLLING OFFICE NAME AND ADDRESS: Defense Contract Administration Services Management Area, Detroit McNamara Federal Bldg., 477 Michigan Avenue Detroit, MI 48226	12. REPORT DATE: August 25, 1983
	13. NUMBER OF PAGES: 9
14. MONITORING AGENCY NAME & ADDRESS (if different from Controlling Office): Office of Naval Research 1030 Green Street Pasadena, CA 91106	15. SECURITY CLASS. (of this report): Unclassified
	15a. DECLASSIFICATION/DOWNGRADING SCHEDULE

16. DISTRIBUTION STATEMENT (of this Report)

Unlimited

17. DISTRIBUTION STATEMENT (of the abstract entered in Block 20, if different from Report)

18. SUPPLEMENTARY NOTES

To be published in the proceedings of the FEL Workshop held at Eastsound, WA, June, 1983.

19. KEY WORDS (Continue on reverse side if necessary and identify by block number)

Free electron laser, two-stage FEL, phase space buckets, phase space displacement, trapping, electron energy spread

approx. to the 7th power to the 8th power 59 cm approx.

20. ABSTRACT (Continue on reverse side if necessary and identify by block number)

Phase space displacement is investigated as a method of reducing energy spread in free electron lasers producing long-wavelength (λ 1 mm) at high laser intensity ($\sim 10^7$-10^8 W/cm^2). The technique is described and compared with the more conventional tapered wiggler that traps electrons in decelerating phase space buckets. A band model is developed to describe the movement of electrons around the phase space buckets and estimate the resulting energy spread. The energy spread obtained from the band model is compared with that obtained from a multi-particle computer simulation. Laser gain obtained by bucket capture is found

DD FORM 1 JAN 73 1473 EDITION OF 1 NOV 65 IS OBSOLETE

SECURITY CLASSIFICATION OF THIS PAGE (When Data Entered)

20.

to be comparable to gain obtained by phase space displacement at high intensities but energy spread is a factor of a few lower.

Limiting energy spread at high laser intensities using phase space displacement

H. Takeda and S. B. Segall

KMS Fusion, Inc., P.O. Box 1567, Ann Arbor, Michigan 48106

Abstract

Phase space displacement is investigated as a method of reducing energy spread in free electron lasers producing long-wavelength radiation (~ 1 mm) at high laser intensity (~ 10^7-10^8 W/cm^2). The technique is described and compared with the more conventional tapered wiggler that traps electrons in decelerating phase space buckets. A band model is developed to describe the movement of electrons around the phase space buckets and estimate the resulting energy spread. The energy spread obtained from the band model is compared with that obtained from a multiparticle computer simulation. Laser gain obtained by bucket capture is found to be comparable to gain obtained by phase space displacement at high intensities but energy spread is a factor of a few lower.

Introduction

KMS Fusion, Inc. is planning to participate in a two-stage FEL experiment to be performed at The University of California Santa Barbara (UCSB) using the UCSB recirculating electrostatic accelerator[1]. To obtain adequate gain to sustain oscillation in the short-wavelength second stage of the FEL, a high-intensity long-wavelength pump field is needed. This long-wavelength pump field is produced by the first stage FEL interaction. For the available current and anticipated cavity losses in the experiment, a pump field intensity on the order of 10^8 W/cm^2 will be needed to produce laser oscillations in the second stage.

For this high pump field intensity, a large energy spread will be produced in the electron beam as it passes through the wiggler magnet. If it is required to collect the electron beam with high efficiency after it leaves the wiggler, this energy spread could represent a serious problem. The return beam line and electron collector in the electrostatic accelerator must be designed to handle the energy spread. The wiggler used to produce the high intensity field must also be designed to minimize the energy spread produced.

In this paper we will investigate an amplifier design that minimizes energy spread at high laser intensity using phase space displacement. We will compare phase space displacement to the standard bucket capture technique for gain optimization. The analysis will show that at high intensities comparable gain can be produced using either method, but that a lower energy spread results from phase space displacement.

Energy spread produced by bucket capture

The bucket formed by the ponderomotive wave can be obtained from the equations of motion for an electron in an FEL[2]. For an electron with an energy near the resonant energy ($\gamma - \gamma_R << \gamma_R$), approximate equations of motion for the electron are

$$\frac{dP}{dt} = -D(\sin \Psi - \sin \Psi_R) \qquad (1)$$

and

$$\frac{d\psi}{dt} = AP \ , \tag{2}$$

where

$$A = c\,(k_L + k_w)\,\frac{1 + a_w^2}{\gamma_R^3} \ , \tag{3}$$

$$D = \frac{\omega_L a_L a_w}{\gamma_R} , \tag{4}$$

$$a_L = \frac{eE_L}{k_L mc^2} \ , \tag{5}$$

$$a_w = \frac{eE_w}{k_w mc^2} \ . \tag{6}$$

$P = \gamma - \gamma_R$, ψ is the phase angle of the electron relative to the ponderomotive wave, and a_L and a_w represent the dimensionless amplitudes of the vector potentials for the laser and wiggler fields respectively. The wave numbers for the laser and wiggler fields are k_L and k_w.

Eliminating the time differential and integrating over ψ, we get

$$P = \sqrt{\frac{2D}{A}\,(\cos\psi + \psi \sin\psi_R + K)} \tag{7}$$

We now choose the value of the integration constant K to give the maximum bound orbit in the region $-\pi < \psi < \pi$. This defines the phase space bucket. For a positive resonant angle ψ_R, the bucket equation is

$$P = \sqrt{\frac{2D}{A}\,\{\cos\psi + \cos\psi_R + (\psi + \psi_R - \pi)\sin\psi_R\}} \quad ; \ 0 < \psi_R < \frac{\pi}{2} \tag{8}$$

The half bucket height is obtained at $(\psi = \psi_R)$. It is proportional to the square root of the laser field amplitude. The electron energy spread will be at least as large as the full bucket height when the electrons in the bucket execute a synchrotron oscillation in the wiggler. When a number of synchrotron oscillations take place in the wiggler, the untrapped electrons drift away from the bucket. The synchrotron oscillation frequency is also proportional to the square root of the laser field amplitide. Figure 1 shows the half bucket height for a wiggler with a 1 kG field on axis plotted against laser intensity for zero resonant phase and a radiation wavelength of 1 mm. For a 3 MeV electron beam the full bucket height at an intensity of $\sim 10^8$ W/cm^2, is about 20% of the electron energy. It would be difficult to transport an electron beam with such a large energy spread without large losses[3].

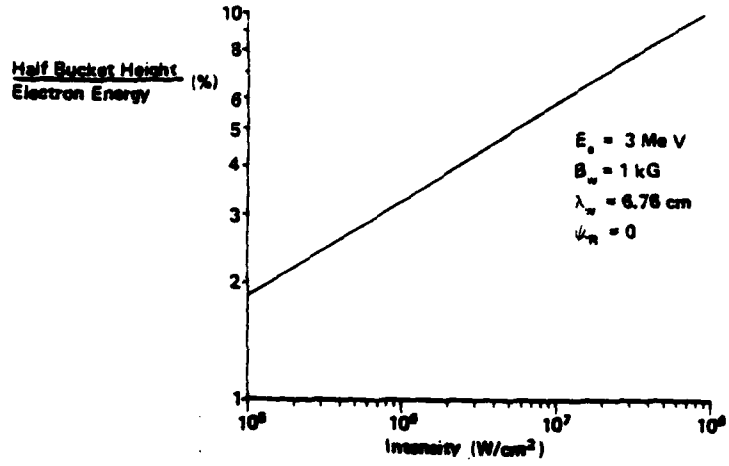

Figure 1. Half bucket height as a function of laser intensity for an FEL producing 1-mm radiation.

Phase space displacement

In contrast to bucket capture, phase space displacement requires an empty bucket. The empty bucket can be accelerated through the electron distribution in phase space using a reverse-tapered wiggler. In a reverse-tapered wiggler, the resonant phase of the bucket is negative and is in the range between 0 and $-\frac{\pi}{2}$. Electrons going around the bucket give up energy to the laser beam. None of the electrons are trapped in the bucket. Alternatively, the wiggler taper could be replaced by an equivalent decelerating axial electric field. The electron beam, which is initially above the bucket, would then be decelerated around the stationary empty bucket by the axial electric field, again transferring energy to the laser beam.

Kroll, Morton and Rosenbluth[4] first considered the application of phase space displacement to the FEL. In their paper, the energy spread of the incoming electron beam was assumed to be much larger than the bucket produced by the ponderomotive wave. In our case the initial energy spread of the electron beam relative to the bucket height is negligible.

In order to move all of the electrons in the distribution around the bucket, a minimum number of synchrotron oscillations must take place in the wiggler. Since the synchrotron oscillation frequency is proportional to the square root of both the laser field amplitude and the wiggler magnetic field, a high laser intensity is required. For a 3 Mev electron beam and 1 kG wiggler field on axis, we need a laser intensity of at least 4×10^6 W/cm^2 to enable all the electrons in the distribution to move below the bucket in a 3-meter-long wiggler designed to produce 1-mm radiation.

Higher order separatrices as extensions of the bucket

To help understanding how electrons move around the bucket we use the concept of higher order separatrices. Higher order separatrices are an extension of the bucket trajectory to phase angles outside the range occupied by the bucket. Figure 2 shows a number of buckets and several higher order separatrices above and below the buckets. These separatrices divide phase space into multiple bands. Once an electron occupies a particular band it stays in that band throughout the wiggler provided the laser gain is low and the buckets do not grow significantly, which will be true at high intensity. Under these conditions the number of bands occupied by the electron beam is a constant of the motion.

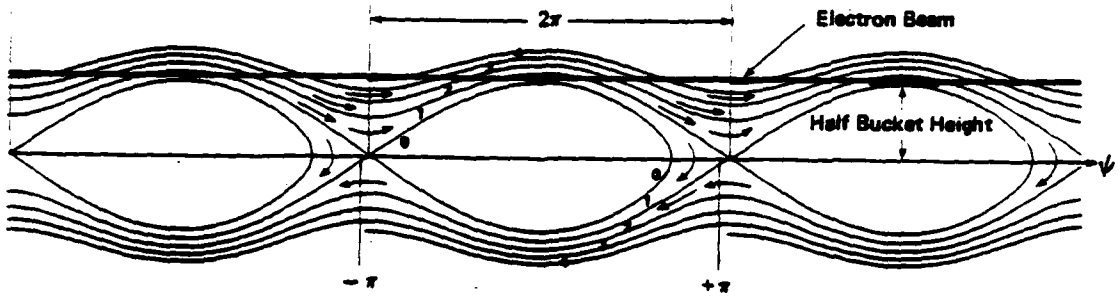

Figure 2. Higher order separatrices divide phase space into multiple bands. These separatrices were obtained for a wiggler with a 1 kG field on axis and a resonant phase $\Psi_R = -4.2^\circ$. The intensity of the 1-mm-wavelength radiation field is 10^8 W/cm^2.

The bucket was defined as the maximum bound orbit of an electron. Higher order separatrices are obtained by continuing the bucket trajectory beyond the unstable fixed point of the bucket. For negative resonant phase angle, we determine the integration constant K for the bucket Equation (7) in the same way as for a positive resonant angle, by finding the value of K for which $P = 0$ at the unstable fixed point, which for negative resonant phase is $\Psi = -\pi - \Psi_R$ in the principal domain $[-\pi < \psi < \pi]$. The bucket equation for a negative resonant angle then becomes

$$P_o = \sqrt{\frac{2D}{A}\left[\cos\Psi + \cos\Psi_R + (\Psi + \Psi_R + \pi)\sin\Psi_R\right]} \quad ; -\frac{\pi}{2} < \Psi_R < 0 \,, \tag{9}$$

Since a bucket is located in every interval of 2π radians along the Ψ axis, we may consider a bucket located in the domain $-(1-2m)\pi < \Psi < (1+2m)\pi$. The continuation of the trajectory for this bucket into the principal domain is then referred to as the m-th order separatrix and is given by

$$P_m = \sqrt{\frac{2D}{A}\left[\cos\Psi + \cos\Psi_R + \left[\Psi + \Psi_R + \pi(1-2m)\right]\sin\Psi_R\right]} \quad ; \quad 0 < m \,. \tag{10}$$

In the principal domain, the higher order separatrices divide the phase space above and below the bucket into multiple bands. Figure 2 shows separatrices up to fourth order.

Only electrons in the band between the bucket and first order separtrix (1st band) have orbits that take them directly around the bucket. Electrons in the band between the (m-1)th and m-th separatrix must pass by m-1 buckets before their trajectories takes them around a bucket and reduce their energy below the resonant energy. Those electrons in the band bounded by the highest order separatrices will require the longest time to move around a bucket. Figure 3 shows the number of bands occupied by a monoenergetic electron distribution with an energy equal to the resonant energy plus the bucket height. The number of bands occupied is seen to decrease rapidly with decreasing resonant phase.

All separatrices P_m have a minimum at $\Psi = -\pi - \Psi_R$. Therefore, for a monoenergetic electron distribution, electrons initially at this resonant phase will be located in the highest band. The value, m_h, for the highest band is the lowest value of m for which

$$P_m(-\psi - \psi_R) > P_o(\psi_R) \quad . \tag{11}$$

Relation (11) was used to obtain the number of occupied bands as a function of resonant phase in Figure 3.

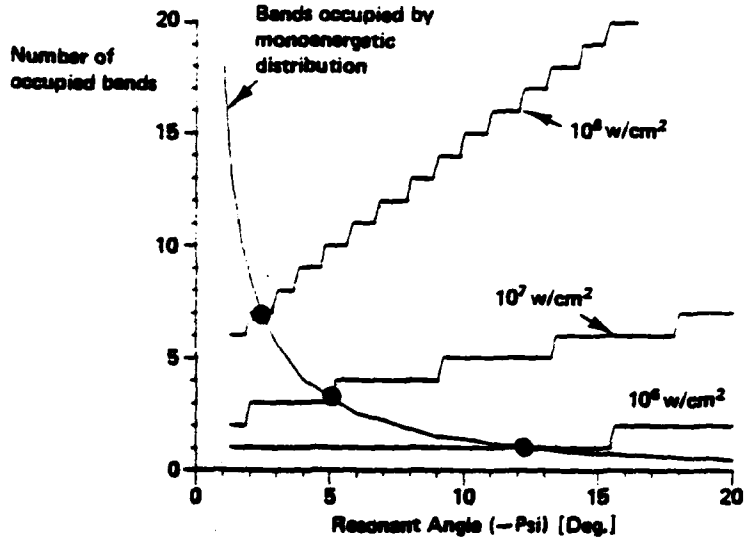

Figure 3. Number of bands occupied by an initially monoenergetic electron distribution tangent to the top of the bucket as a function of resonant phase angle. The difference between the staircase curves and the curve for a monoenergetic distribution represents the number of bands electrons will descend below the bucket in the principal domain while passing through the wiggler. The number of bands is a function of laser intensity and resonant angle. Steps represent transitions between bands. The intersection of the staircase curves with the curve for the number of occupied bands gives the threshold resonant phase angle. The example is for a 3-m-long 1 kG-field wiggler producing 1-mm radiation with a 3-meV electron beam.

Rather than viewing the electron distribution as occupying several bands in the principal domain, we can view the electron distribution as occupying a single band over an extended phase domain containing several buckets. If the electrons occupy m bands in the principal domain, the same distribution can be represented as a series of beamlets occupying a single band over $2\pi m$ radians. In order for all of the electrons in a monoenergetic distribution to go from an energy equal to the resonant energy plus the bucket height to an energy equal to or less than the resonant energy, the entire train of beamlets must move through this extended phase domain. The time required for this to happen is the time required for the beamlet farthest from the bucket to reach and move around the bucket. The energy spread at this time will equal the difference in energy between the first and last beamlet in the extended phase domain.

To estimate the time required for the electron distribution to move around a bucket we substitute the expression for P_m in Equation (10) into Equation (2) giving

$$\frac{d\psi}{dt} = \Delta P = \sqrt{2DA\left[\cos\psi + \cos\psi_R + \{\psi + \psi_R + \pi(1-2m)\}\sin\psi_R\right]} \quad . \tag{12}$$

Integrating (17) assuming negligible gain we obtain

$$\tau(m) = \frac{1}{\sqrt{2\eta A}} \int_{-\pi-\Psi_R}^{\pi-\Psi_R} d\Psi \left[\cos\Psi + \cos\Psi_R + \{\Psi + \Psi_R + \pi(1-2m)\}\sin\Psi_R\right]^{-1/2} \tag{13}$$

$$= \frac{1}{\sqrt{2\eta A}} F(m,\Psi_R)$$

The integration is taken from $-\pi - \Psi_R$ to $\pi - \Psi_R$ because we wish to determine the transit time of the particles in the highest band. These particles are located around $-\pi - \Psi_R$ in the principal domain. All the dimensioned quantities are contained in the term preceding the integral

$$\frac{1}{\sqrt{2\eta A}} = \gamma^2 \left[2\omega_L a_L a_W c(k_L + k_W)(1 + a_W^2)\right]^{-1/2}$$

$$= \frac{\lambda_W}{4\pi c}\sqrt{\frac{1 + a_W^2}{2a_L a_W}} \tag{14}$$

By making the substitution $u = \Psi + \Psi_R$ the dimensionless term becomes

$$F(m,\Psi_R) = \int_{-\pi}^{\pi} du \left[\cos(u - \Psi_R) + \cos\Psi_R + \{u + \pi(1-2m)\}\sin\Psi_R\right]^{-1/2} \qquad (m > 1)\ . \tag{15}$$

For the bucket (m = 0) we get

$$F(0,\Psi_R) = \int_{-\pi}^{(\Psi_1 + \Psi_R)} du \left[\cos(u - \Psi_R) + \cos\Psi_R + (u + \pi)\sin\Psi_R\right]^{-1/2}\ . \tag{16}$$

where Ψ_1 is the value of Ψ for which $P = 0$ for a bucket in the interval $[0, \pi/2]$. Figure 4 shows $F(m,\Psi_R)$ as a function of m for a number of different values of the resonant phase angle.

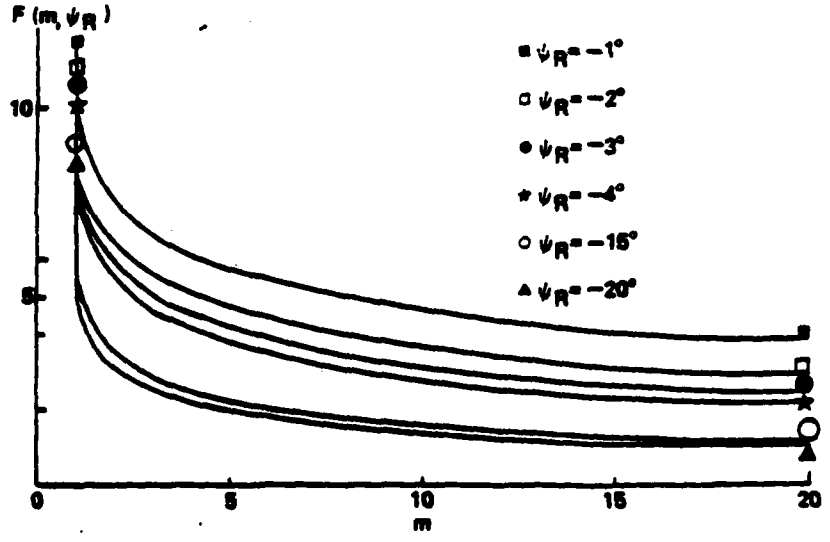

Figure 4. Graph of $F(m,\Psi_R)$ as a function of m for different values of Ψ_R.

The time required for an electron initially located in a band between two separatrices at the phase $-\pi - \Psi_R$ to go from its initial energy to the resonant energy is approximately the same as the time required for an electron located on the separatrix above it to reach the resonant energy. This time is given by

$$\tau(m,\Psi_R) = \sum_{j=1}^{m} \frac{1}{\sqrt{2DA}} F(j,\Psi_R)$$

$$= \frac{\lambda_w}{4\pi c} \sqrt{\frac{1 + a_w^2}{2a_L a_w}} F_s(m,\Psi_R) \tag{17}$$

where

$$F_s(m,\Psi_R) = \sum_{j=1}^{m} F(j,\Psi_R) \tag{18}$$

The actual time the electron beam interacts with the wiggler magnet is given by

$$\tau_w = \frac{N\lambda_w}{\beta_z c} = \frac{N\lambda_w}{c} \tag{19}$$

where N is the number of periods in the wiggler. In order for the electron distribution to move around the bucket during the time it is in the wiggler we must have

$$\tau_w > \tau(m_h,\Psi_R) \tag{20}$$

or

$$F_s(m_h,\Psi_R) < 4\pi N \sqrt{\frac{2a_L a_w}{1 + a_w^2}} \tag{21}$$

When $\tau_w = \tau(m_h,\Psi_R)$, (This equation was used to obtain the staircase curves of Figure 3.) electrons from the highest band just succeed in reaching the resonant energy. For a given laser intensity this condition provides a threshold value for the resonant phase angle required to utilize phase space displacement for reducing energy spread. These threshold values are shown for three different laser intensities in Figure 3.

At intensities for which phase space displacement is advantageous for reducing energy spread, the electrons in the highest band not only decrease their energy to the resonant energy, but continue to move below the bucket. To estimate the energy spread produced in the wiggler we must calculate how far below the bucket electrons, initially in the highest band, have moved by the time they reach the end of the wiggler. Since the equation for the separatrices are symmetric above and below the bucket

$$\tau_w = \frac{1}{\sqrt{2DA}} F_s(m_h,\Psi_R) + \frac{1}{\sqrt{2DA}} \sum_{j=1}^{n} F(j,\Psi_R) \tag{22}$$

τ_w and F_s can be determined, so equation (22) can be solved for n, the number of bands, electrons, initially in the highest band, have descended below the bucket by the time they reach the end of the wiggler. In most cases Equation (22) will not be satisfied for an integral value of n. Performing a numerical integration we can determine the fraction of a band needed to satisfy Equation (22).

To estimate the energy spread we assume electrons initially in the first band move down the same number of bands as electrons initially in the highest occupied band. Using Equation (10) we can then estimate the final energies for the highest and lowest bands. The values for energy spread obtained using this band model can be compared with the values for energy spread obtained from a multiparticle simulation of an electron beam in the wiggler. This is shown in Figure 5 for the 3-m-long wiggler we have been considering with a laser intensity of 10^7 W/cm^2. Agreement is reasonably good except at low absolute values of the resonant phase, which are below the threshold value necessary for electrons in the highest band to reach the resonant energy (see Figure 3). There is a good deal of scatter in the simulation results below this threshold value, as would be expected. The dip in the energy spread for the band model calculation between -9 and -10 degrees resonant phase results from electrons in the highest band crossing from one band to the next. The simulation is insensitive to this artifact of the band model calculation. A similar comparison of energy spreads obtained from the band model and multiparticle simulations at a laser intensity of 10^8 W/cm^2 is shown in Figure 6. Agreement is not as good as in Figure 5, but demonstrates the same qualitative behavior. Values for energy spread obtained using phase space displacement are compared with those obtained from bucket capture in Figure 7. All results were obtained using a multipaticle simulation. For the proper choice of resonant phase, determined in Figure 7 by the axial voltage gradient, it is possible to reduce the energy spread significantly using phase space displacement. Figure 8 compares laser gain produced using phase space displacement with gain obtained by bucket capture. Again the results are from simulation calculations in which an axial electric field rather than a wiggler taper was assumed. Phase space displacement results are shown only for axial electric fields corresponding to resonant phases above the threshold values. For the range of values calculated, gain produced by phase space displacement is comparable to or greater than the gain produced by trapping.

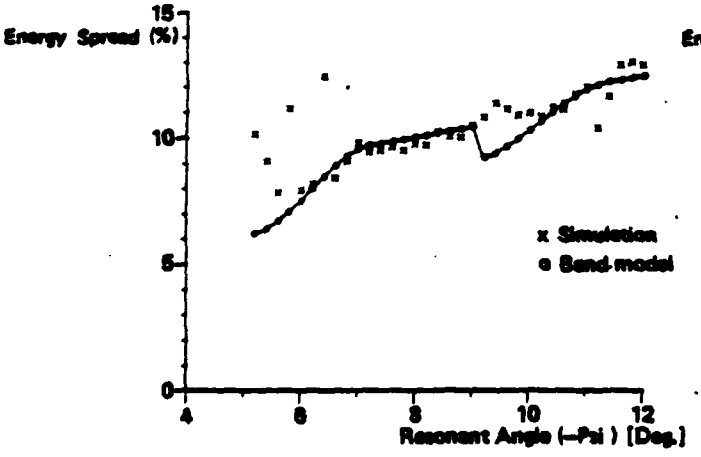

Figure 5. Energy spread as a function of resonant phase at a laser intensity of 10^7 W/cm^2 calculated using both a multiparticle simulation and the band model.

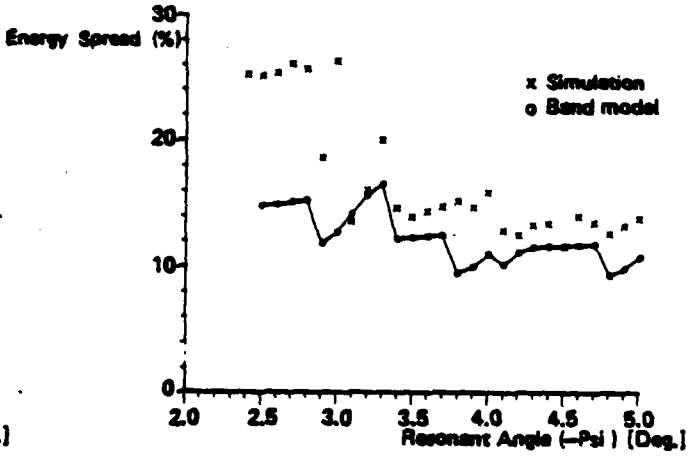

Figure 6. Energy spread as a function of resonant phase at a laser intensity of 10^8 W/cm^2.

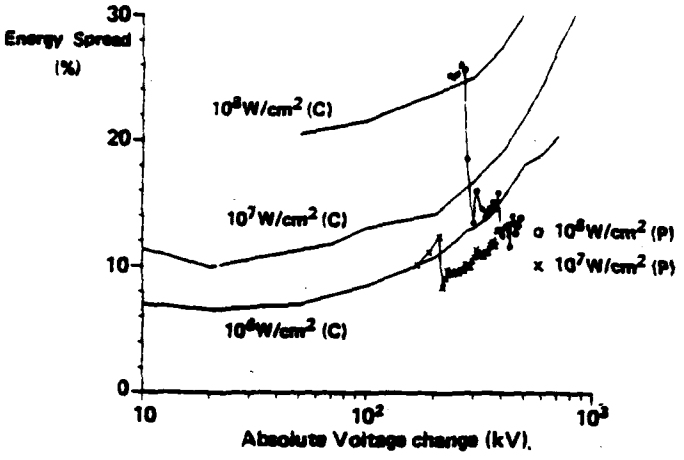

Figure 7. Energy spread as a function of absolute voltage change across a 3-m wiggler using phase space displacement (P) and bucket capture (C) for a number of different laser intensities.

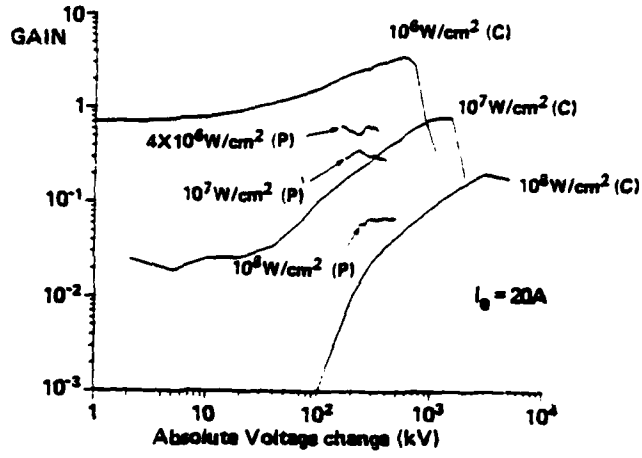

Figure 8. Laser gain as a function of absolute voltage change across a 3-m wiggler for phase space displacement (P) bucket capture (C).

Conclusions

We are required to operate a long-wavelength free electron laser at very high intensities (~10^8 W/cm^2) as the first stage of a two-stage FEL. This produces a large energy spread in the wiggler than makes collection of the electron beam in a electrostatic accelerator difficult. To reduce this energy spread we have investigated using phase space displacement rather than bucket capture to optimize the laser gain. We have seen that whereas decelerating trapped electrons in phase space buckets results in a total electron energy spread that is larger than the full bucket height, using phase space displacement the energy spread could be reduced to the order of half the bucket height with no significant loss of gain.

Acknowledgment

This work was supported by the United States Office of Naval Research.

References

1. L. R. Elias and G. Ramian, "UCSB FEL Electron Beam System" in Physics of Quantum Electronics, Volume 9, Jacobs, Pilloff, Scully, Sargent, and Spitzer editors, Addison-Wesley (1982).

2. W. R. Fiddleston and S. R. Segall, "Equations of Motion for a Free-Electron Laser with an Electromagnetic Pump Field and an Axial Electrostatic Field", IEEE Journal of Quantum Electronics, QE-17, 1488 (1981).

3. M. Takeda and S. R. Segall, "Amplification Optimization Study for an FEL Wiggler with a Helical Magnetic Field and an Axial Electric Field", IEEE Transactions on Nuclear Science, NS-30, 3112 (1983).

4. N. M. Kroll, P. L.Morton and M. N. Rosenbluth, "Free-Electron Lasers with Variable Parameter Wigglers", IEEE Journal of Quantum Electronics, QE-17, 1436 (1981).

Director
Defense Advanced Research Projects Agency
(3 copies)
Attn: Technical Library
1400 Wilson Boulevard
Arlington, VA 22209

Office of Naval Research
(3 copies)
Physics Division Office (Code 412)
800 North Quincy Street
Arlington, VA 22217

Office of Naval Research
Director, Technology (Code 200)
800 North Quincy Street
Arlington, VA 22217

Naval Research Laboratory
(3 copies)
Department of Navy
Attn: Technical Library
Washington, DC 20375

Office of the Director of Defense Research and Engineering
(3 copies)
Information Office Library Branch
The Pentagon
Washington, DC 20301

U.S. Army Research Office
(2 copies)
Box 1211
Research Triangle Park, NC 27709

Defense Technical Information Center
(12 copies)
Cameron Station
Alexandria, VA 22314

Director, National Bureau of Standards
Attn: Technical Library
Washington, DC 20234

Commanding Officer
(3 copies)
Office of Naval Research Western Detachment Office
1030 East Green Street
Pasadena, CA 91101

Commanding Officer
(3 copies)
Office of Naval Research Eastern/Central Detachment Office
495 Summer Street
Boston, MA 02210

Commandant of the Marine Corps
Scientific Advisor (Code RD-1)
Washington, DC 20380

Naval Ordnance Station
Technical Library
Indian Head, MD 20640

Naval Postgraduate School
Technical Library (Code 5632.2)
Point Mugu, CA 93010

Naval Ordnance Station
Technical Library
Louisville, KY 40214

Commanding Officer
Naval Ocean Research & Development Activity
Technical Library
NSTL Station, MS 39529

Naval Explosive Ordnance Disposal Facility
Technical Library
Indian Head, MD 20640

Naval Ocean Systems Center
Technical Library
San Diego, CA 92152

Naval Surface Weapons Center
Technical Library
Silver Springs, MD 20910

Naval Ship Research & Development Center
Central Library (Code L42 and L43)
Bethesda, MD 20084

Naval Avionics Facility
Technical Library
Indianapolis, IN 46218


FIL
10